Manuscript ID: 1815
DOI: 10.18462/iir.icr.2019.1815

# Experimental Study on a Water and Air Source High-Temperature Heat Pump Using a Low GWP Refrigerant

**Choyu Watanabe[(a), (b)], Toshiyuki Nakamura[(a)], Motoki Yamada[(a)], Tomoyuki Yamada[(a)], Atsuki Hattori[(a)], Tadayoshi Aono[(a)], Shuto Tomita[(a)]**

(a) Graduate School of Engineering of Nagoya University
Nagoya, 463-8603, Japan, watanabe.choyu@ng.mbox.nagoya-u.ac.jp
(b) Chubu Electric Power Co., Inc.
Nagoya, 459-8522, Japan, Watanabe.Chouyuu@chuden.co.jp

## ABSTRACT

A high-temperature heat pump using a low GWP refrigerant, such as R1234yf or R454C, were experimentally investigated to supply hot water. The temperature of hot water ranged from 45 °C to 90 °C for R1234yf and ranged from 45 °C to 75 °C for R454C, while the temperature of supplied water ranged from 6 °C to 24 °C. The temperature of heat sources ranged from 7 °C to 25 °C. Degrees of sub-cooling of sub-critical heat pump cycles ranged from 10 °C to 70 °C because large temperature-rise was needed to heat supplied water. A test apparatus and measurement system were presented. The test results using R1234yf and a water-source evaporator were discussed in comparison with the test results of the former work using R1234yf and an air-source evaporator. The test results using R1234yf and a water-source evaporator were discussed in comparison with the test results using R454C.
Keywords: Low GWP Refrigerant, R1234yf, R454C, COP, Energy Efficiency

## 1. INTRODUCTION

Heat pump technology is important to boost the reduction of $CO_2$ emissions, reduce primary energy consumption and increase the amount of renewable energy usage due to high energy efficiency of heat pumps. To further enhance these effects, the development and spread of high temperature heat pumps for hot water supply and re-heating of hot water circulation must be supported. For example, air source heat pumps using R134a as a refrigerant for re-heating hot water circulation have been applied to cutting and washing processes in automobile parts factories (Watanabe, 2017).
The low GWP refrigerants, such as R1234yf and R454C, are expected as the next generation refrigerants for heat pumps. A water source high-temperature heat pump using R1234yf (Watanabe et al., 2017) and an air source high-temperature heat pump using R1234yf (Watanabe et al., 2018) has been investigated. However, heating capacity and heating COP did not reach expected values. Because evaporation temperature could not be controlled properly with a thermostatic expansion valve with internal pressure equalization due to the pressure drop in distributors to a plurality of refrigerant passages of an air source evaporator.
In this paper, a water source high-temperature heat pump using R1234yf or R454C with thermostatic expansion valves with external pressure equalization are experimentally investigated to supply hot water. A test apparatus and measurement system are presented. Test results using R1234yf and a water source evaporator are discussed in comparison with the test results of the former work using R1234yf and an air source evaporator (Watanabe et al., 2018). The test results using R454C and a water source evaporator are discussed in comparison with the test results using R1234yf.

## 2. REFRIGERANTS FOR HIGH-TEMPERATURE HEAT PUMPS

Properties of refrigerants for high-temperature heat pumps are shown in Table 1. GWP (100 years), safety, critical pressure, critical temperature and boiling point temperature of each refrigerant are described for R1234yf, R1234ze(E), R454C, R32, R410A, R134a and R290 in this table. R454C is composed of R1234yf (78.5 mass%) and R32 (21.5 mass%). When we selected refrigerants in this

paper, we though the refrigerants to be removed, whose GWP (100 years) is higher than 150, or whose flammability is high. Further, we thought the refrigerants to be removed, whose boiling point temperature is higher than -25 °C because the lowest evaporation temperature of a sub-critical cycle is -25 °C, assumed that the lowest temperature of heat source air is -15 °C and the lowest evaporation temperature is lower by 10 K than the temperature of heat source air. R1234yf and R454C were selected because they were not removed.

**Table 1. Properties of refrigerants for high-temperature heat pumps**

| Classification | Refrigerant | Chemical formula | $GWP_{100}$ | Safety [3] | Critical point | | Boiling point[4] (°C) |
|---|---|---|---|---|---|---|---|
| | | | | | Pressure (M Pa) | Temperature (°C) | |
| HFO | R1234yf | $CF_3CF=CH_2$ | <1[1] | A2L | 3.38 | 94.7 | -29.5 |
| | R1234ze(E) | Trans-$CHF=CHCF^3$ | <1[1] | A2L | 3.64 | 109.4 | -19.0 |
| HFO & HFC | R454C | - | 146[1] | A2L | 4.69 | 88.5 | -45.9 |
| HFC | R32 | $CH_2F_2$ | 677[1] | A2L | 5.78 | 78.1 | -51.7 |
| | R134a | $CF_3CH_2F$ | 1,300[1] | A1 | 4.06 | 101.1 | -26.1 |
| Natural refrigerant | R290 | $C_3H_8$ | 3[2] | A3 | 4.24 | 106 | -42.1 |

1) Values of Global Warming Potential 100 year according to Appendix 8.A, the 5th final report of IPCC WG1.
2) Values of Global Warming Potential 100 year for R290 according to Table 2.15, IPCC Fourth Assessment Report.
3) A: lower toxicity, B: higher toxicity, 1: no flame propagation, 2L: lower flammability with a maximum burning velocity of ≤10 cm/s, 2: lower flammability with a maximum burning velocity of >10 cm/s, 3: higher flammability classified according to ISO 817:2014.
4) Temperature at which the liquid boils under standard atmosphere, 0.1013 MPa.

## 3. EXPERIMENTAL APPARATUS FOR HIGH-TEMPERATURE HEAT PUMPS

Figure 1 shows the schematic drawing of an experimental apparatus for high-temperature heat pump and measure points. Figure 2 shows the outside view of the apparatus. The apparatus consists of a refrigerant circuit of a heat pump cycle, heat sink water circuit to measure heating capacity and heat source water circuit to use a water source evaporator. The refrigerant circuit consists of a compressor, a water-cooled condenser, a receiver, a water-cooled sub-cooler, two expansion valves for R1234yf and R454C, an air-source evaporator with a fan, a water-source evaporator, an accumulator and sight glasses. The condenser, sub-cooler and water-source evaporator are all copper-brazed stainless-steel plate type heat exchangers. The receiver is arranged between the condenser and the sub-cooler. The semi-hermetic reciprocating compressor 2KES-05Y made by Bitzer was adopted. The compressor has two cylinders, a bore diameter of 30 mm, a stroke of 33 mm and a displacement volume of 490 $m^3$/h when the frequency of power source is 60 Hz. The maximum discharge pressure is 3.2 MPa, and the maximum suction pressure is 1.9 MPa. The compressor has a 3-phase 200V induction motor, which has a maximum output of 1.8 kW. The heat sink water circuit consists of a heat sink water tank, an auxiliary chiller, a heat sink water pump driven by an inverter and a fan coil unit. The inner volume of the heat sink water tank is 0.035 $m^3$. Supplied water is heated in the sub-cooler and condenser. The heat of hot water is dissipated to ambient air in the fan coil unit. The heat source water circuit consists of a heat source water tank, a heat source water pump driven by an inverter, and a heat exchanger between heat source water and heat sink water. The inner volume of the heat source water tank is 0.035 $m^3$.

Refrigerant pressure was measured with piezo-resistance pressure transducers. Refrigerant temperature was measured with copper-constantan thermo-couples attached on outside surfaces of copper tubes in which refrigerant flows. Mass flow rate of refrigerant was measured with a Coriolis flowmeter. Water temperature was measured with platinum resistor temperature sensors inserted in the water pipes. Flow rate of water was measured with two electromagnetic flowmeters.

## 4. EXPERIMENTAL CONDITIONS

Experimental conditions of the former work (Watanabe et al., 2018) are shown in Table 2 according to JIS C 9220-2011. Dry bulb air temperature, wet bulb air temperature, water supply temperature and hot water temperature are shown for each season condition in Table 2. Figure 3 shows the air-source evaporator and thermostat expansion valve with internal pressure equalization of the former work (Watanabe et al., 2018). Heating capacity and heating COP did not reach expected values. Because evaporation temperature could not be controlled properly with a thermostatic expansion valve with internal pressure equalization due to the pressure drop in distributors to a plurality of refrigerant passages of an air source evaporator. Experimental conditions of this work are shown in Table 3. Source water temperature, water supply temperature and hot water temperature are shown for each season condition in Table 3. Maximum hot water temperature is 75 °C for R454C while that is 90 °C for R1234yf. Because the critical temperature of R454C is lower than that of R1234yf. Figure 4 shows the water-source evaporator and thermostat expansion valve with external pressure equalization newly adopted in this work to enable proper control of expansion.

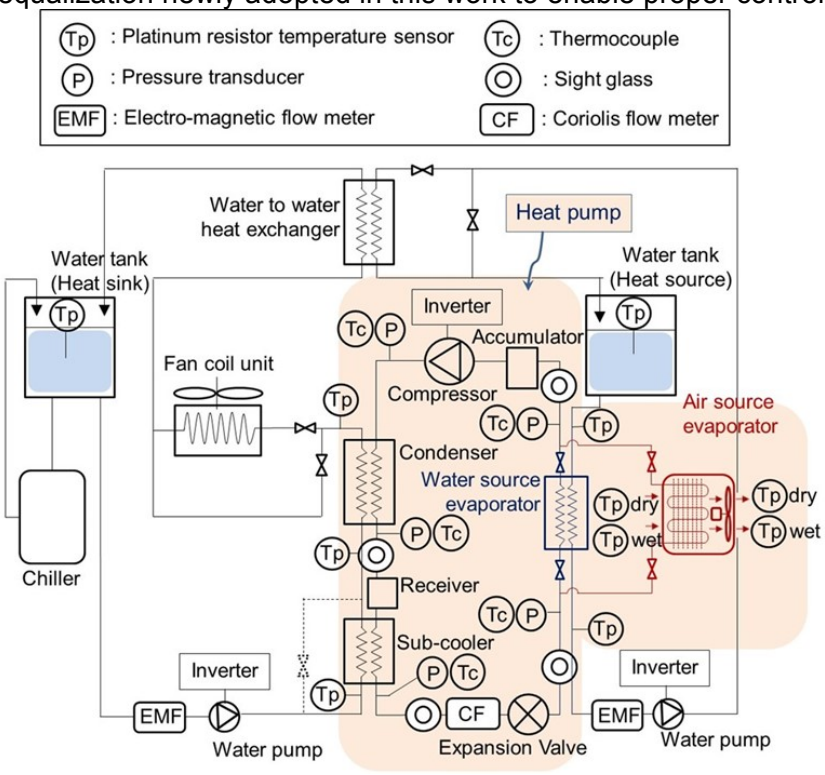


**Figure 1: Schematic drawing of an experimental apparatus and measure points**

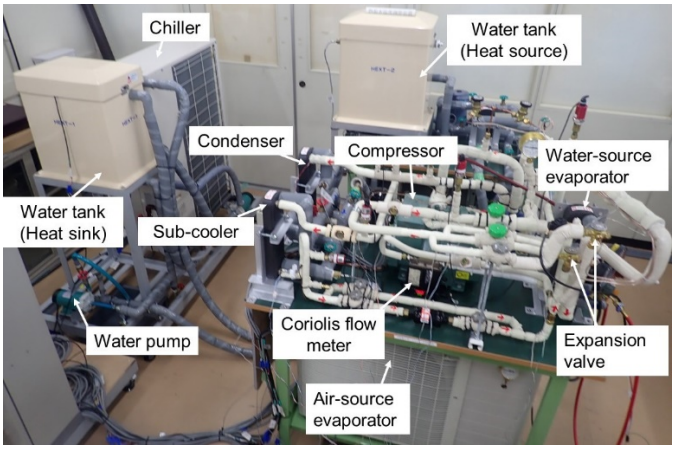


**Figure 2: Outside view of an experimental apparatus for high-temperature heat pumps**

**Table 2. Experimental conditions (R1234yf air-source heat pump) (Watanabe et al., 2018)**

| Season | Heat source air temperature (°C, dry bulb) | Heat source air temperature (°C, wet bulb) | Water supply temperature (°C) | Hot water temperature (°C) |
|---|---|---|---|---|
| Summer | 25 | 21 | 24 | 45, 65, 80, 90 |
| Midterm | 16 | 12 | 17 | 45, 65, 80, 90 |
| Winter | 7 | 6 | 9 | 45, 65, 80, 90 |
| Frost | 2 | 1 | 5 | 45, 65, 80, 90 |

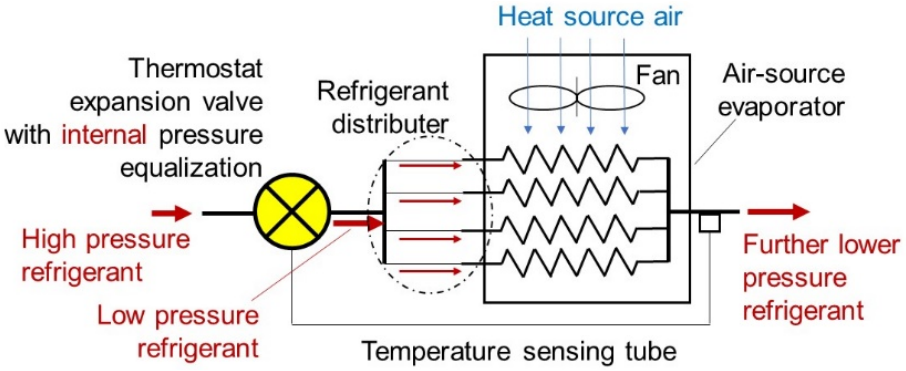


**Figure 3: Air-source evaporator and thermostat expansion valve with internal pressure equalization (Watanabe et al., 2018)**

**Table 3. Experimental conditions (water-source heat pump)**

| Season | Heat source water temperature (°C) | Water supply temperature (°C) | Hot water temperature (°C) | |
|---|---|---|---|---|
| | | | R1234yf | R454C |
| Summer | 25 | 24 | 45, 65, 80, 90 | 45, 65, 75 |
| Midterm | 16 | 17 | 45, 65, 80, 90 | 45, 65, 75 |
| Winter | 7 | 9 | 45, 65, 80, 90 | 45, 65, 75 |

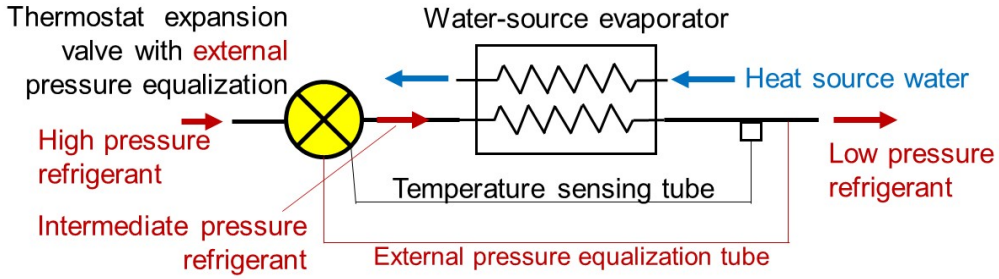


**Figure 4: Water-source evaporator and thermostat expansion valve with external pressure equalization**

## 5. EXPERIMENTAL RESULTS AND DICCUSSION

Fig. 5 shows heating COP versus hot water temperature (45 °C, 65 °C, 80 °C and 90 °C) and heating capacity versus hot water temperature for each season condition. Square marks show the test results using R1234yf, the water-source evaporator and thermostat expansion valve with external pressure equalization obtained in this work. And solid lines show approximate curves obtained from experiment points. Circle marks show the test results using R1234yf, the air-source evaporator and thermostat expansion valve with internal pressure equalization obtained in the former work (Watanabe et al., 2018). And dashed lines show approximate curves obtained from the experiment points. Blue marks and lines show the test results and approximate curves under the summer condition. Orange marks and lines show the test results and approximate curves under the midterm condition. Grey marks and lines show the test results and approximate curves under the winter condition. Heating capacities and heating COPs obtained in this work are larger than those obtained in the former work. The increase of heating capacities and heating COPs are the largest under the

summer condition, the median under the midterm condition and the smallest under the winter condition.

Fig. 6, Fig. 7 and Fig. 8 shows pressure–enthalpy diagrams and temperature–entropy diagrams of the heat pump cycles drawn using CYCLE_D (Brown, J.S. et al., 2009). Red marks and lines show the heat pump cycles using R1234yf, the water-source evaporator and thermostat expansion valve with external pressure equalization obtained in this work. Blue marks and lines show the test results using R1234yf, the air-source evaporator and thermostat expansion valve with internal pressure equalization obtained in the former work (Watanabe et al., 2018). Fig. 6 shows the test results under the summer condition and hot water temperature 45 °C. Fig. 7 shows the test results under the midterm condition and hot water temperature 65 °C. Fig. 8 shows the test results under the midterm condition and hot water temperature 90 °C. In all cases of Fig. 6, Fig. 7 and Fig. 8, evaporation pressures and evaporation temperatures rise in the heat pump cycles obtained in this work in comparison with the heat pump cycles obtained in the former work. The rise of evaporation pressure and temperature shows the largest value in Fig. 6, the median value in Fig. 7 and the smallest value in Fig. 8. Because the mass flow rate of the refrigerant is the largest value and the evaporation pressure of the refrigerant is the lowest in Fig. 6; the mass flow rate of the refrigerant is the median value and the evaporation pressure of the refrigerant is the median value in Fig. 7; the mass flow rate of the refrigerant is the smallest value and the evaporation pressure of the refrigerant is the largest in Fig. 8.

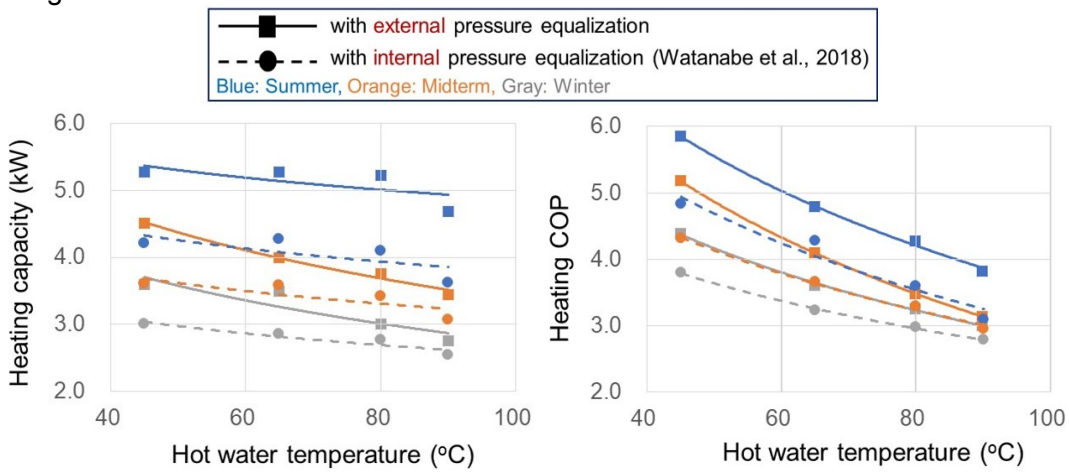


**Figure 5: Experimental data regarding heating capacity and heating COP for hot water temperature**

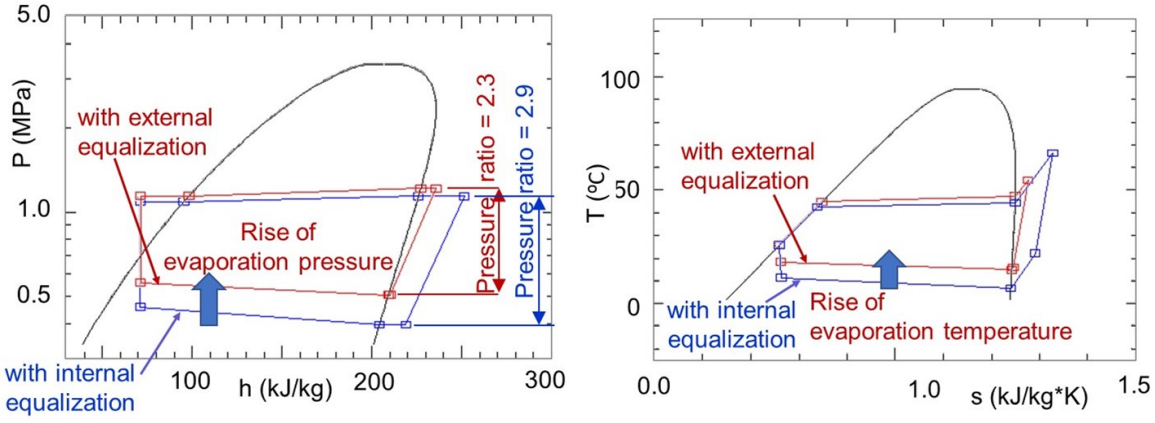


**Figure 6: P-h and T-s diagrams (R1234yf, summer, hot water temperature: 45 °C)**

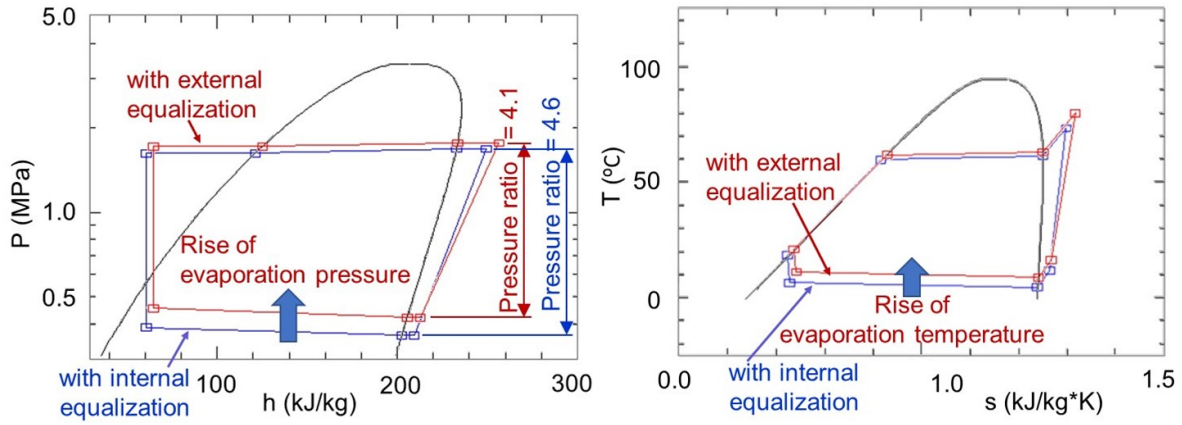


**Figure 7: P-h and T-s diagrams (R1234yf, midterm, hot water temperature: 65 °C)**

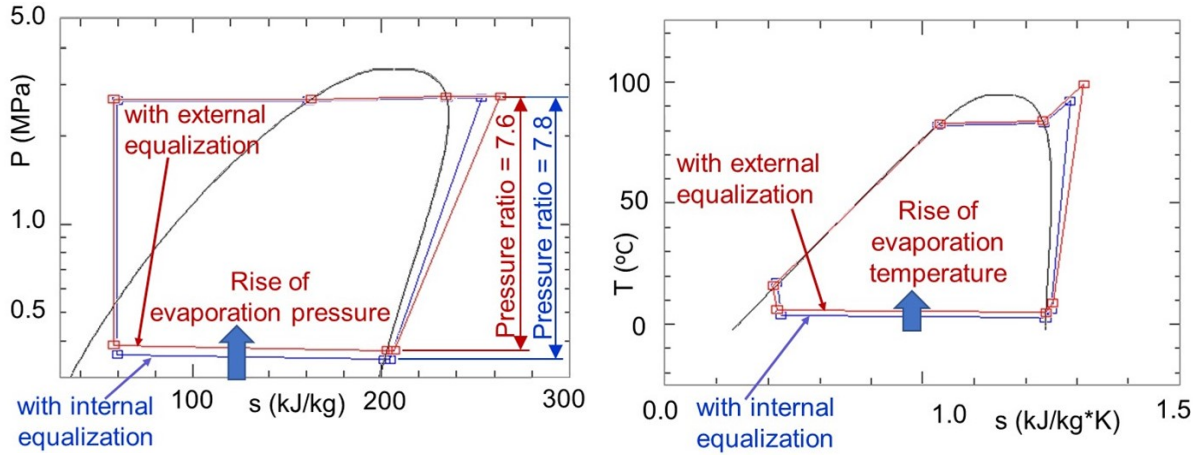


**Figure 8: P-h and T-s diagrams (R1234yf, winter, hot water temperature: 90 °C)**

Fig. 9 shows heating COP versus hot water temperature (45 °C, 65 °C and 75 °C for R454C; 45 °C, 65 °C, 80 °C and 90 °C for R1234yf) and heating capacity versus hot water temperature for each season condition. Square marks show the test results using R454C, the water-source evaporator and thermostat expansion valve with external pressure equalization obtained in this work. And solid lines show approximate curves obtained from experiment points. Circle marks show the test results using R1234yf, the water-source evaporator and thermostat expansion valve with external pressure equalization obtained in this work. And dashed lines show approximate curves obtained from the experiment points. Blue marks and lines show the test results and approximate curves under the summer condition. Orange marks and lines show the test results and approximate curves under the midterm condition. Grey marks and lines show the test results and approximate curves under the winter condition. Heating capacities of R454C are larger than those of R1234yf. However, heating COPs of heat pump cycles using R454C are smaller than those of R1234yf because the heating capacities and cooling capacities of R454C are larger than those of heat pump cycles using R454C R1234yf using the same condenser and evaporator.

Fig. 10-12 shows pressure–enthalpy diagrams and temperature–entropy diagrams of the heat pump cycles drawn using CYCLE_D (Brown, J.S. et al., 2009). Red marks and lines show the heat pump cycles using R454C, the water-source evaporator and thermostat expansion valve with external pressure equalization obtained in this work. Blue marks and lines show the test results using R1234yf, the water-source evaporator and thermostat expansion valve with external pressure equalization obtained in this work. Fig. 10 shows the test results under the summer condition and hot water temperature 45 °C. Fig. 11 shows the test results under the midterm condition and hot water temperature 65 °C. Fig. 12 shows the test results under the midterm condition and hot water temperature 75 °C for R454C, and 90 °C for R1234yf. In both cases of Fig. 10 and Fig. 11, condensation and evaporation pressures of R454C are higher than those of R1234yf in the heat

pump cycles while condensation and evaporation temperatures of R454C are approximately equal to those of R1234yf. In Fig. 12, condensation pressures and evaporation temperatures of R454C are approximately equal R1234yf while evaporation pressures and condensation temperatures of R454C are higher than those of R1234yf.

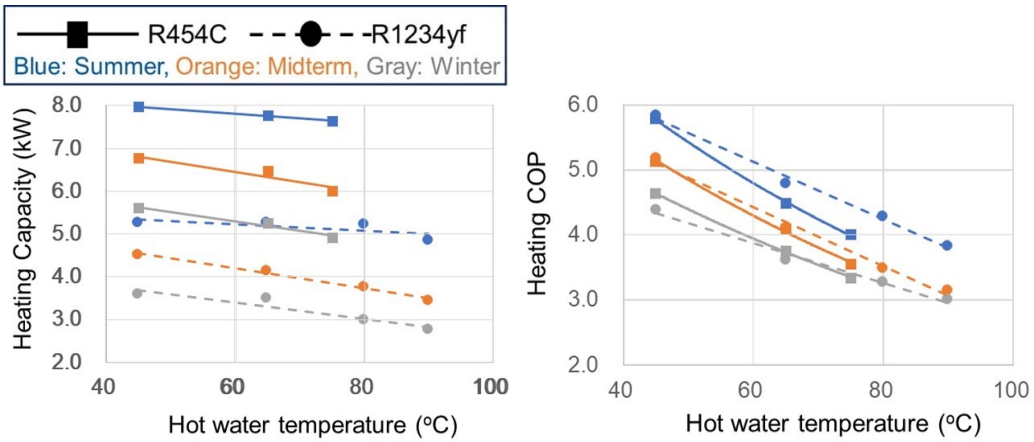


**Figure 9: Experimental data regarding heating capacity and heating COP for hot water temperature**

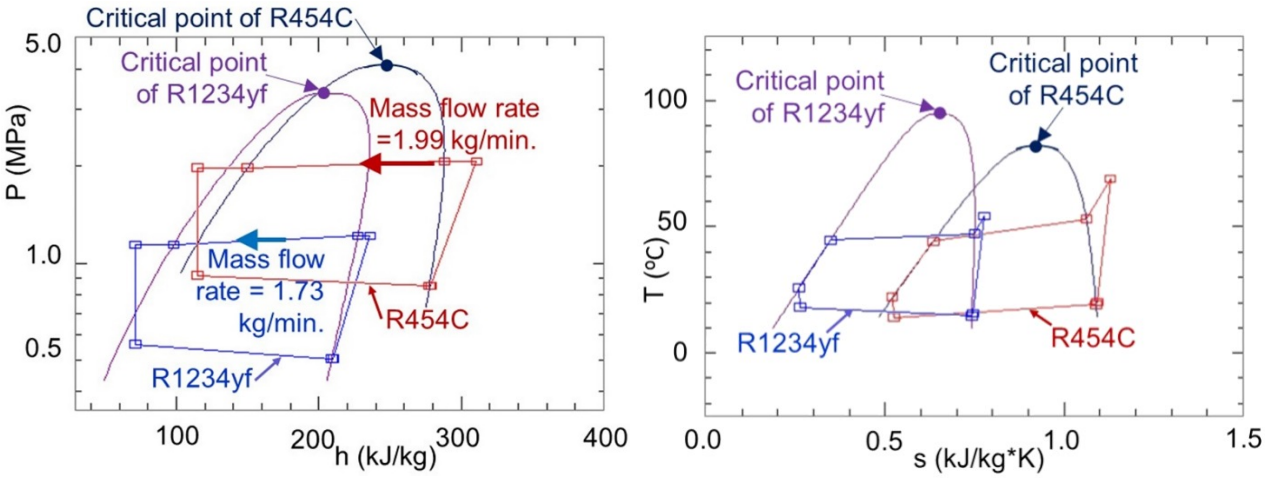


**Figure 10: P-h and T-s diagrams (summer, hot water temperature: 45 °C)**

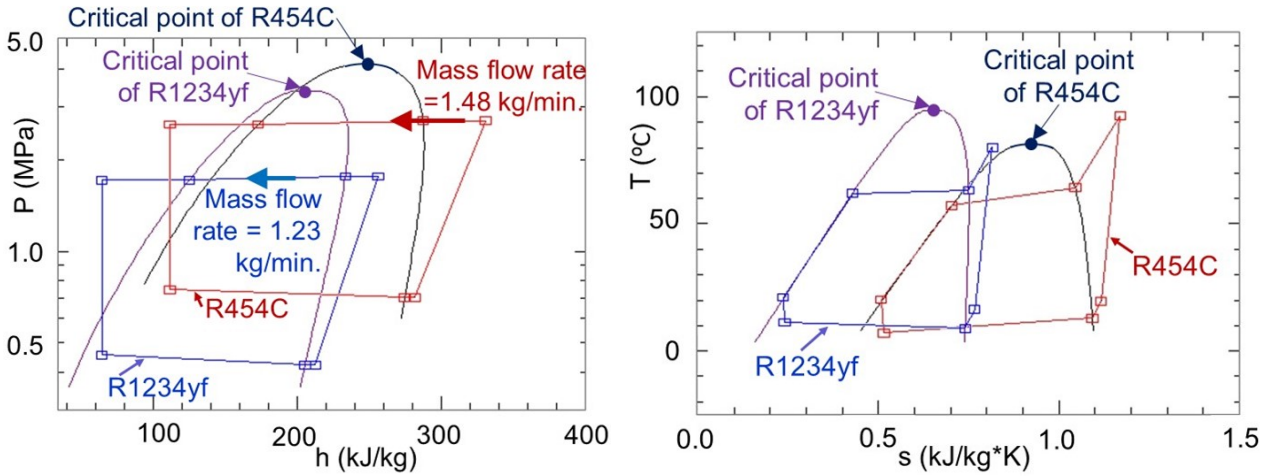


**Figure 11: P-h and T-s diagrams (midterm, hot water temperature: 65 °C)**

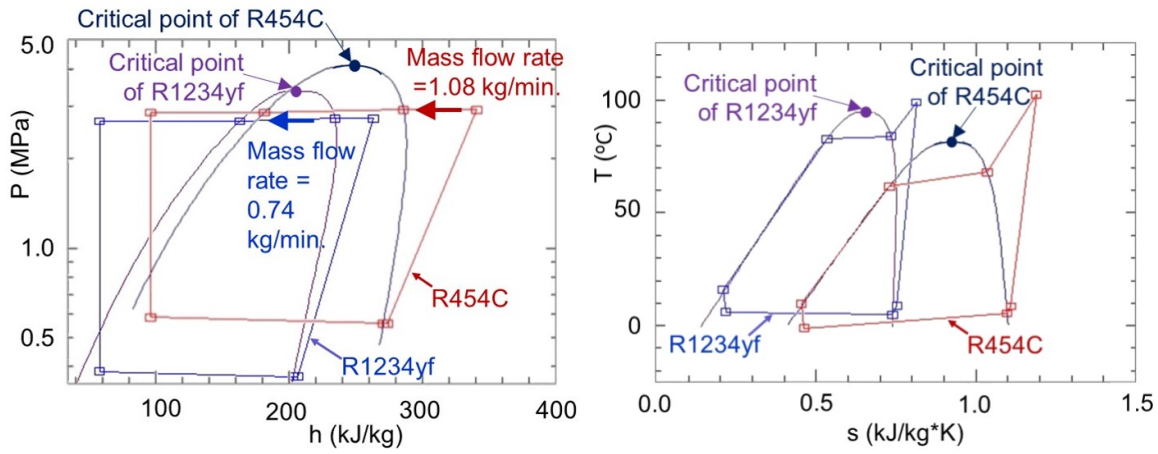


**Figure 12: P-h and T-s diagrams (winter, hot water temperature: 75 °C for R454C, 90 °C for R1234yf)**

## 6. CONCLUSIONS

The high-temperature heat pump using a low GWP refrigerant, such as R1234yf or R454C, were experimentally investigated to supply hot water. The temperature of hot water ranged from 45 °C to 90 °C for R1234yf and ranged from 45 °C to 75 °C for R454C, while the temperature of supplied water ranged from 6 °C to 24 °C.

Heating capacities and heating COPs obtained using R1234yf and a thermostat expansion valve with external pressure equalization are larger than those obtained using R1234yf and a thermostat expansion valve with internal pressure equalization.

Heating capacities of heat pump cycles using R454C are larger than those of heat pump cycles using R1234yf. However, heating COPs of heat pump cycles using R454C are smaller than those of heat pump cycles using R1234yf because the heating capacities and cooling capacities of R454C are larger than those of R1234yf using the same condenser and evaporator.


## ACKNOWLEDGEMENTS

This study has been conducted as Creative Experiments for Comprehensive Engineering of Graduate School of Engineering of Nagoya University.


## NOMENCLATURE

| | | | |
|---|---|---|---|
| $P$ | pressure (MPa) | $h$ | specific enthalpy (kJ×kg$^{-1}$) |
| $T$ | temperature (°C) | $s$ | specific entropy (kJ×kg$^{-1}$×K$^{-1}$) |

## REFERENCES


Watanabe, C., 2017, Application of Heat Pumps to Cutting and Washing Processes, European Heat Pump Summit 2017, No. 3.

Watanabe, C. et al., 2017. Theoretical and Experimental Study on Air-source High-Temperature Heat Pumps Using a Low GWP Refrigerant. Proceedings of the 9th Asian Conference on Refrigeration and Air-conditioning, Japan Society of Refrigerating Air conditioning Engineers, o.3.3.2.

Watanabe, C. et al., 2018. Theoretical and Experimental Study on High-Temperature Heat Pumps Using a Low GWP Refrigerant. Proceedings of the 12th Heat Pump Conference 2017, International Energy Agency, A325.

Brown, JS et al., 2009. CYCLE_D: NIST Vapor Compression Cycle Design Program -Version 5.0 (NIST Standard Reference Database 49).